# Mixed Order Tangential Vector Finite Elements (TVFEs) for Tetrahedra and Applications to Multi-Functional Automotive Antenna Design

**Tutku Karacolak and Erdem Topsakal**

Department of Electrical and Computer Engineering
Mississippi State University,
Mississippi State, MS 39762, USA

***Abstract*** — Mixed order tangential vector finite elements (TVFEs) of order 0.5, 1.5, and 2.5 for tetrahedra are presented and used in conjunction with an exact Finite Element-Boundary Integral (FE-BI) formulation. The main advantage of using mixed order elements is to reduce the computational complexity when solving large problems. As an illustrative example, a wide band antenna is designed and placed on an automobile. Results regarding the antenna return loss, far field pattern, axial ratio, and gain are presented.

## I. INTRODUCTION

Printed microstrip patch antennas are widely used in wireless communications because they are low profile, low cost, and can easily be integrated with other circuitry. However, conventional patches find very few applications due to their narrow bandwidth. In the past, techniques have been proposed to overcome this bandwidth problem by using parasitic patches, stacked patches, and thick substrates [1]-[2]. Despite the advantages, these methods enlarge the antenna size either in the antenna plane or in the antenna height. Some other patch antennas investigated include E-shaped, spiral, tapered slot, and bow-tie [3]-[6]. E-shaped and square slot antennas are preferred for wideband and multi-band operations. They have been used in mobile and satellite communications, remote sensing, electronic warfare, and radar systems [7]-[10].

Another important application area is the design of multi-functional automotive antennas. Nowadays, satellite radio, navigation, and personal communication systems are standard features in many automobiles. These applications require a compact circularly polarized wideband antenna with decent gain and omni-directional characteristics. In this study, we propose the design of such antenna by using a square slot with an E-shaped tuning stub. The antenna has less than -10 dB return loss in the 0.8 GHz -3.35 GHz band and can be used for GPS, XM, GSM, and PCS systems. FE-BI software is used for simulations. Initial antenna results are validated with Ansoft's HFSS. In addition, the antenna is placed on the automobile and simulations are carried out to observe the changes in the antenna parameters in the presence of the automobile.

## II. FORMULATION

The finite element method boundary integral method (FE-BI) is known to be very accurate when analyzing antennas with fine geometrical details [11]. Using tetrahedral elements offers higher flexibility when simulating complex structures, and mixed-order tangential vector finite elements (TVFEs) guarantee tangential field continuity across element boundaries and suppress spurious modes [12].

In the past, mixed order TVFEs are proposed up to $1.5^{th}$ order for a patch antenna backed by a dielectric filled rectangular cavity recessed in infinite ground plane [13]. Formulation used in [13] omits the edge effects and determines the unknown magnetic currents on the boundary and the electric fields inside the finite element domain. It is obvious that for a general radiation problem involving a complex structure such formulation will easily fail. An alternative exact formulation was introduced in [14]. In this formulation the FE-BI system is of the form

$$\begin{bmatrix} E_{vv} & E_{vs} & 0 \\ E_{sv} & E_{ss} & S \\ 0 & K & L \end{bmatrix} \begin{bmatrix} E_v \\ E_s \\ J \end{bmatrix} = \begin{bmatrix} V_v \\ V_s \\ V_j \end{bmatrix} \tag{1}$$

where $E_v$ refers to the electric fields in the interior volume of the antenna and $E_s$ is the sub-column for the surface fields. The $J$ sub-column of unknowns contains the current density unknowns on the large metallic surface of the sub-structure. In the given system, the sub-matrices $E_{ss}$, $E_{vv}$, $E_{sv}$, and $E_{vs}$ are sparse and can thus be treated efficiently in the context of an iterative solver. Their explicit form is known [14]. The time harmonic electric field is related to the time-dependent electric field by $\mathsf{E}(x,y,z;t) = \Re e\left\{\vec{E}(x,y,z)e^{jwt}\right\}$ where $j = \sqrt{-1}$. They are extracted by discretizing the functional

$$F(\mathrm{E})=\frac{1}{2}\int_v\left[\frac{1}{\mu_r}(\nabla\times\vec{E})\cdot(\nabla\times\vec{E})-k_0^2\varepsilon_r\vec{E}\cdot\vec{E}\right]dv\,. \quad (2)$$

For Magnetic Field Integral Equation (MFIE) formulation, the elements of the matrix in (1) are obtained from the operators

$$L=\int_s ds\ \ \vec{t}(\vec{r})\cdot\left[\int_{s'} ds'\overline{G}(\vec{r},\vec{r}')\cdot\vec{M}(\vec{r}')\right] \quad (3)$$

$$K=\int_s ds\ \ \vec{t}(\vec{r})\cdot\left[\frac{1}{2}\vec{J}(\vec{r})+\int_{s'} ds'\vec{J}(\vec{r}')\times\nabla g(\vec{r},\vec{r}')\right] \quad (4)$$

where

$$\overline{G}(\vec{r},\vec{r}')=\left(\bar{I}+\frac{1}{k_0{}^2}\nabla\nabla'\right)g(\vec{r},\vec{r}') \quad (5)$$

and

$$g(\vec{r},\vec{r}')=\frac{e^{-jk_0|\vec{r}-\vec{r}'|}}{|\vec{r}-\vec{r}'|}\,. \quad (6)$$

Finally, the elements of the coupling matrix are obtained from

$$S=-ik_0\int_s(\vec{E}\times\vec{H})\cdot\hat{n}ds. \quad (7)$$

### *Elements and Basis Functions*

We consider a tetrahedral element with nodes 1, 2, 3, and 4. The volume of the tetrahedron is denoted by V. The simplex coordinates $\xi_1$, $\xi_2$, $\xi_3$, and $\xi_4$ at a point P are defined in the usual manner, where $V_n$ denotes the volume of the tetrahedron formed by P and the nodes of the triangular face opposite to node *n* (Fig. 1).

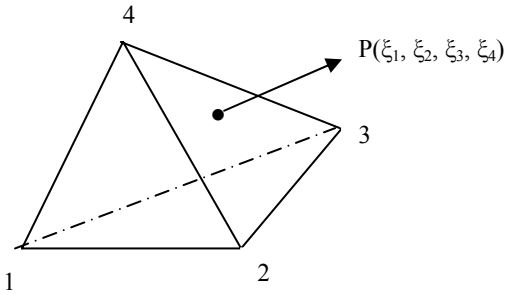


Fig. 1. Geometry of a tetrahedral element.

A mixed-order TVFE of order 0.5 is characterized by six linearly independent vector basis functions which are expressed as

$$\xi_i\nabla\xi_j-\xi_j\nabla\xi_i\ ,i<j\,. \quad (8)$$

A mixed order TVFE of order 1.5 is characterized by 20 linearly independent vector basis functions in a hierarchical fashion. In addition to the six edge-based vector functions (8), it is characterized by the six edge-based vector basis functions

$$(\xi_i-\xi_j)(\xi_i\nabla\xi_j-\xi_j\nabla\xi_i)\ ,\ i<j \quad (9)$$

and the eight face-based vector basis functions

$$\xi_k(\xi_i\nabla\xi_j-\xi_j\nabla\xi_i)\ ,\ i<j<k \quad (10)$$

$$\xi_j(\xi_k\nabla\xi_i-\xi_i\nabla\xi_k)\ ,\ i<j<k\ . \quad (11)$$

A mixed order TVFE of order 2.5 is characterized by 45 linearly independent vector basis functions in a hierarchical fashion. In addition to the 12 edge-based vector functions (8)-(9) and eight face-based vector functions (10)-(11), it is characterized by the six edge-based vector basis functions

$$(\xi_i-\xi_j)^2(\xi_i\nabla\xi_j-\xi_j\nabla\xi_i)\ ,\ i<j \quad (12)$$

16 face-based vector basis functions

$$\nabla(\xi_i\xi_j\xi_k)\ ,\ i<j<k \quad (13)$$

$$\xi_k^2(\xi_i\nabla\xi_j-\xi_j\nabla\xi_i)\ ,\ i<j\ ,\ i\neq j\neq k\neq i \quad (14)$$

and the three cell-based vector basis functions

$$\xi_j\xi_k(\xi_1\nabla\xi_i-\xi_i\nabla\xi_1),\ \ i,j,k>1\ ,\ i\neq j\neq k\neq i\ ,\ \ j<k\ . \quad (15)$$

## III. ANTENNA GEOMETRY

The top and side views of the antenna are shown in Fig. 2a and Fig. 2b, respectively. The antenna consists of a square slot placed between two substrates of the same material.

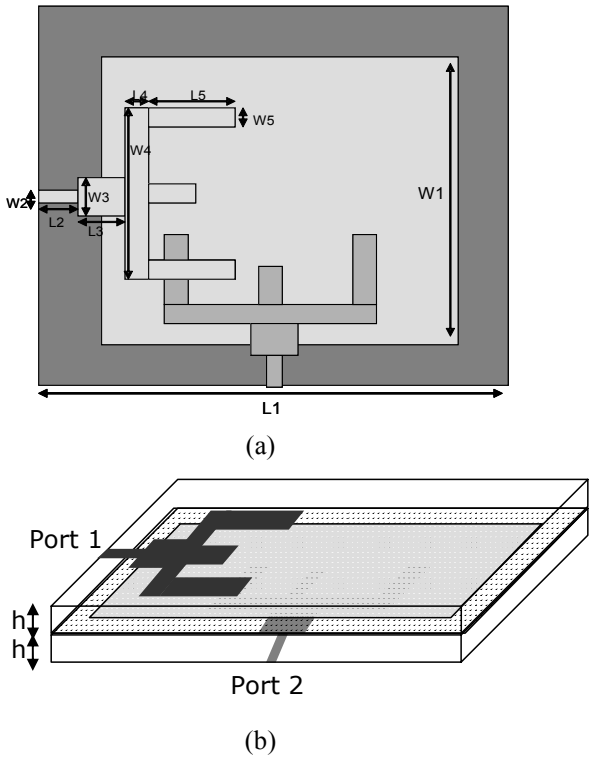


Fig. 2. a) Top and b) Side view of the antenna.

Two E-shaped patches are printed orthogonally (one on the top and one on the bottom of the antenna) and connected to two orthogonal microstrip feed lines. Through proper selection of the parameters of the E-shaped tuning stub, it is expected that the coupling between the microstrip line and the printed wide slot can be controlled more effectively. When dimensions of the E-shaped tuning stub change, the coupling changes and the antenna has different resonance characteristics.

The design maintains a high degree of polarization isolation and employs a symmetric feeding structure. The antenna is a bi-directional radiator, and the radiation patterns on both sides are approximately the same. Moreover, circular polarization is obtained by simultaneous excitation. Neltec NH 9300 ($\varepsilon_r$=3, tanδ=0.0023) with a thickness of 1.27 mm is used for the substrate material. The dimensions of the antenna and the antenna specifications are given in Table 1 and Table 2, respectively. Antenna was designed using a trial-and-error approach.

Table 1. The dimensions of the designed antenna.

| | Antenna Dimensions |
|---|---|
| L1 | 75 mm |
| L2 | 6 mm |
| L3 | 8.5 mm |
| L4 | 3 mm |
| L5 | 12 mm |
| L6 | 6 mm |
| W1 | 57 mm |
| W2 | 1.18 mm |
| W3 | 5 mm |
| W4 | 33 mm |
| W5 | 3 mm |
| h | 1.27 mm |

## IV. NUMERICAL RESULTS

### *A. Square Slot Antenna*

The return loss comparison of the antenna between FE-BI method and HFSS for Port 1 is shown in Fig. 3. Both simulations have very similar characteristics. The HFSS simulation show that the antenna operates in the band 0.8 GHz – 3.35 GHz with a 10 dB bandwidth of 123%. Similarly, according to FE-BI result the band extends from 0.74 GHz to 3.02 GHz with a bandwidth of 121%. Thus, it can be used for GPS (1.227 GHz and 1.575 GHz), XM (2.332 GHz-2.345 GHz), GSM (890 MHz-915 MHz and 935 MHz-960 MHz), and PCS (1.85 GHz-1.99 GHz and 2.18 GHz-2.20 GHz) bands. All FE-BI simulations are done by using 1.5 and 2.5 order elements throughout the entire finite element domain.

Table 2. Square slot antenna specifications.

| | **Antenna Specifications** |
|---|---|
| **Frequency Range** | 0.8 GHz–3.35 GHz |
| **Impedance** | 50 ohms |
| **Return Loss** | Less than -10 dB |
| **Polarization** | Circular |
| **Axial Ratio** | Less than 3 dB |
| **Gain** | 2 dB |
| **VSWR(min performance)** | Less than 2:1 Nominal |

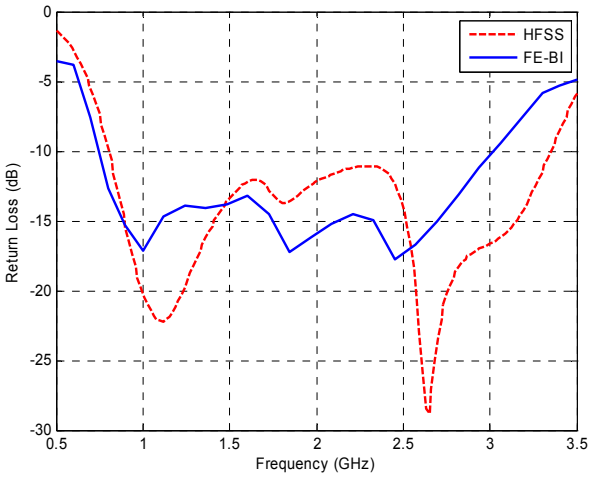


Fig. 3. Return loss of the antenna for Port 1.

S11 and S22 are also very similar due to the symmetry of the ports as shown in Fig. 4. The VSWR and the peak gain of the antenna when only Port 1 is excited are shown in Fig. 5 and Fig. 6. The VSWR level is below "2" throughout the entire band, and reasonable gain flatness around 2 dB is obtained until 2.8 GHz.

Figure 7 shows the calculated axial ratio of the antenna. The antenna provides circular polarization in two bands of 0.8 GHz - 1.9 GHz and 2.8 GHz - 3.35 GHz with 3 dB bandwidths of 95% and 25%, respectively. Axial ratios computed on the x-z and y-z planes at GPS frequencies

(1.227 GHz and 1.575 GHz) are shown in Fig. 8a and Fig. 8b. The axial ratio is less than 3 dB around the z-axis which is the main direction of radiation.

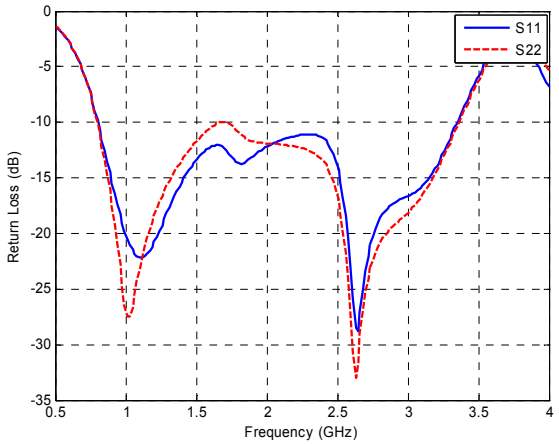


Fig. 4. S11 and S22.

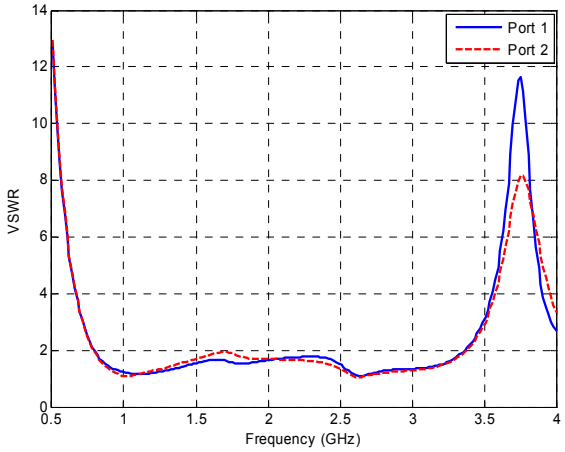


Fig. 5. VSWR for both ports.

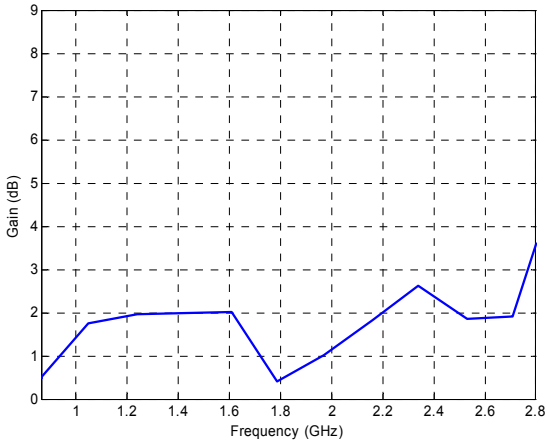


Fig. 6. Peak gain when only Port 1 is excited.

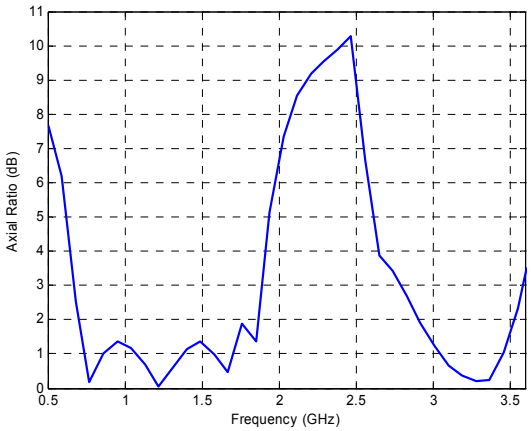


Fig. 7. Axial ratio.

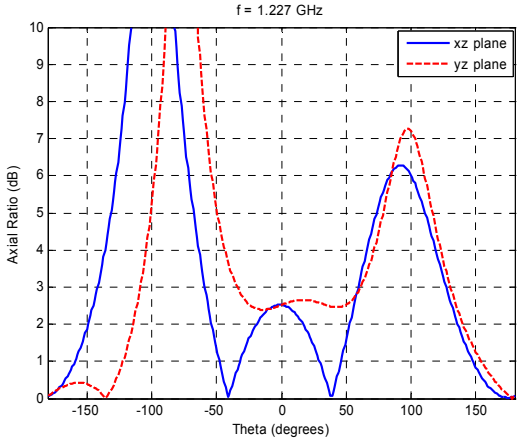


(a)

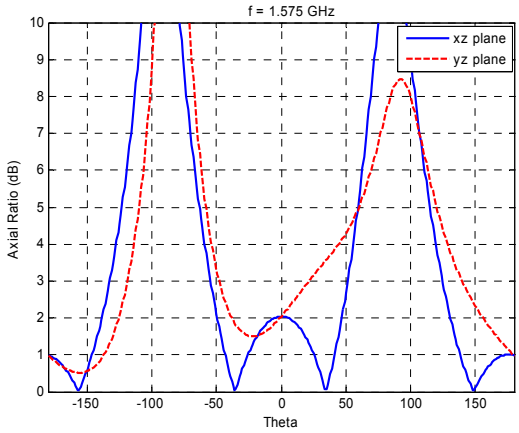


(b)

Fig. 8. Axial ratio on (x-z) and (y-z) planes at a) 1.227 GHz and b) 1.575 GHz.

Figure 9 shows the far field radiation patterns of the antenna on the x-z and y-z planes. E-phi and E-theta components for both planes are calculated at 0.8 GHz, 1.575 GHz, 2.34 GHz, and 3 GHz. It is apparent from the plots that the antenna has omni-directional radiation

characteristics. The cross polarized fields deteriorate as the frequency increases.

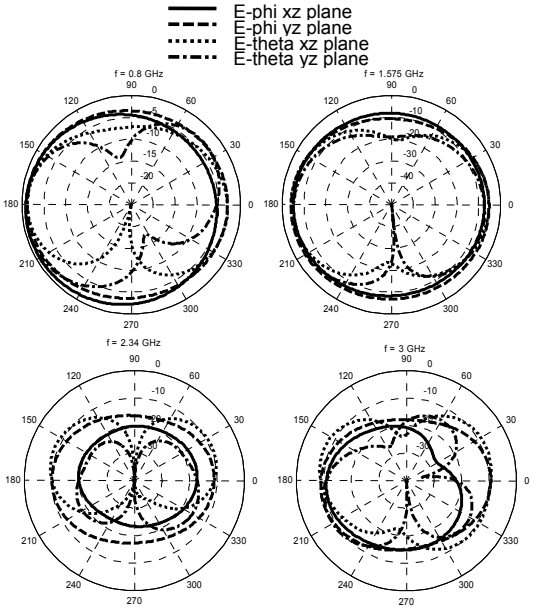


Fig. 9. Radiation patterns of the antenna shown in Fig. 2 on x-z and y-z planes at 0.8 GHz, 1.575 GHz, 2.34 GHz, and 3 GHz.

### *B. Automotive Applications*

Figure 10a, Fig. 10b, Fig. 10c, and Fig. 10d show the antenna on the roof, trunk, 4-door automobile, and convertible automobile meshes, respectively. The length, width, and height of the problems at 3 GHz are also given. In order to reduce the number of unknowns 0.5 order elements are used for the regions further away from the antenna while 1.5 and 2.5 order elements are employed in the vicinity of the antenna.

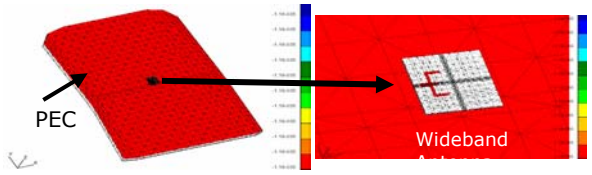


Length=19.5λ Width=10.8λ Height=1.1λ @ 3 GHz

(a)

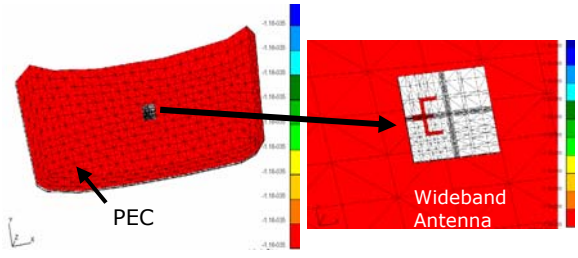


Length=6.2λ Width=14.8λ Height=2.2λ @ 3 GHz

(b)

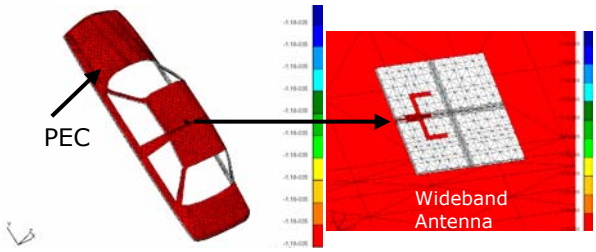


Length=41λ Width=15.4λ Height=7λ @ 3 GHz

(c)

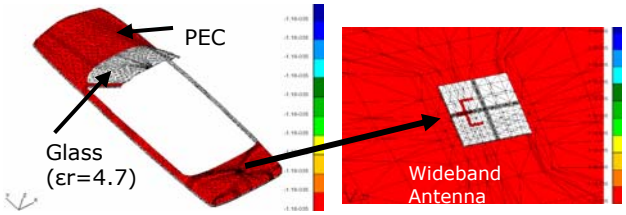


Length=41λ Width=15.4λ Height=7λ @ 3 GHz

(d)

Fig. 10. Square slot antenna on the a) Roof, b) Trunk, c) Whole 4-Door Automobile, and d) Whole Convertible Automobile.

Table 3 shows the number of FE and BI unknowns and total solution time for each problem when combination of 0.5 and 2.5 order elements, and 2.5 order elements alone, are used. The residual error is kept constant for both solutions. BICGSTAB ($l$) algorithm is used for the iterative solver which is superior to other solvers for antenna analysis [15]. As clearly seen from Table 3, mixed order elements improve the solution time and reduces the memory. In BICGSTAB ($l$) algorithm $l$=4 is used for the simulations. In addition, the convergence characteristics of each problem are shown in Fig. 11, Fig. 12, Fig. 13, and Fig. 14, respectively.

Table 3. The number of FE and BI unknowns and total solution time for each problem.

| | **Total FE Unknowns** | **Total BI Unknowns** | **Total Solution Time (sec)** |
|---|---|---|---|
| **Roof** | 5473 (0.5+2.5)<br>37,825 (2.5) | 4880 (0.5+2.5)<br>14,362 (2.5) | 2,664<br>52,872 |
| **Trunk** | 4,721(0.5+2.5)<br>30,523(2.5) | 3,860 (0.5+2.5)<br>11,312(2.5) | 9,636<br>73,467 |
| **4-Door Automobile** | 9,756(0.5+2.5)<br>67,312(2.5) | 11,400(0.5+2.5)<br>33,113(2.5) | 4,3450<br>123,543 |
| **Convertible Automobile** | 10688(0.5+2.5)<br>74,561(2.5) | 10980(0.5+2.5)<br>32,452(2.5) | 24,491<br>137,687 |

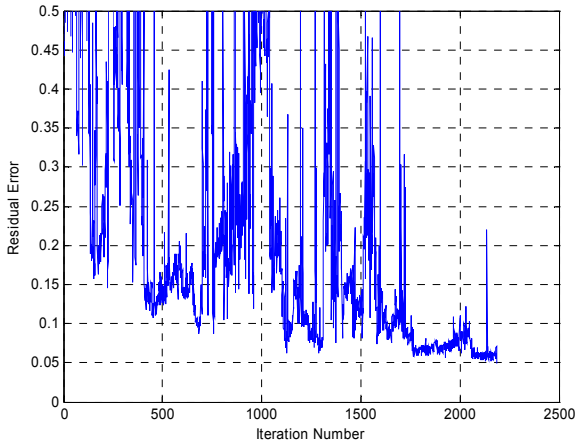


Fig. 11. Convergence behavior of the antenna on the roof.

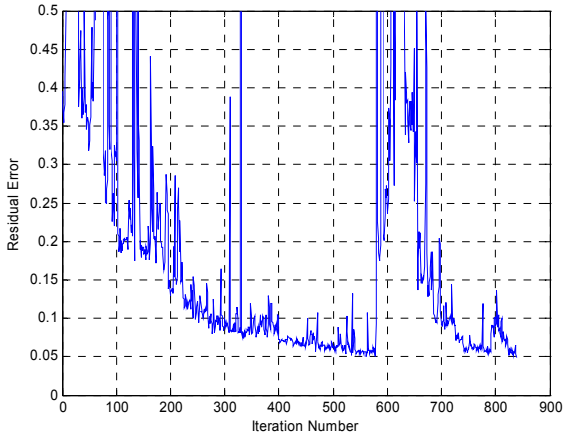


Fig. 12. Convergence behavior of the antenna on the trunk.

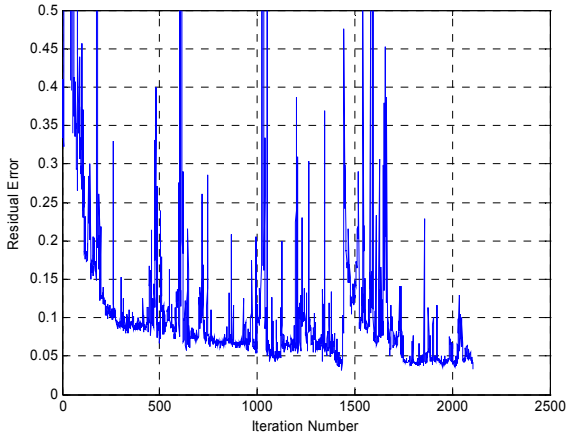


Fig. 13. Convergence behavior of the antenna on the 4-Door automobile.

Figure 15 and Fig. 16 show the similar radiation characteristics of the antenna and the antenna on the roof and on the trunk at GPS, respectively. Although the co-polarization levels for the antenna on the roof and trunk are lower than the antenna alone, the difference is very small around the main direction of radiation (z-axis). Moreover, the cross polarization levels of the antenna on the trunk are lower than the antenna.

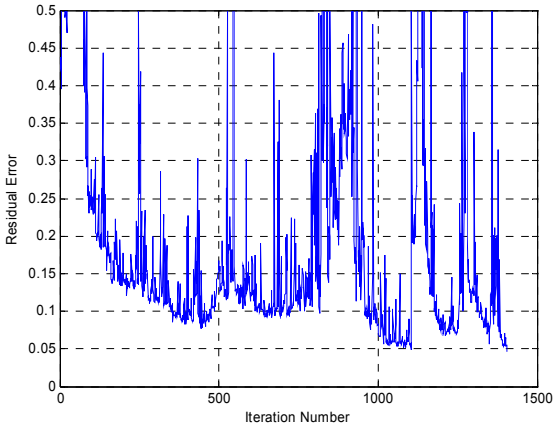


Fig. 14. Convergence behavior of the antenna on the convertible automobile.

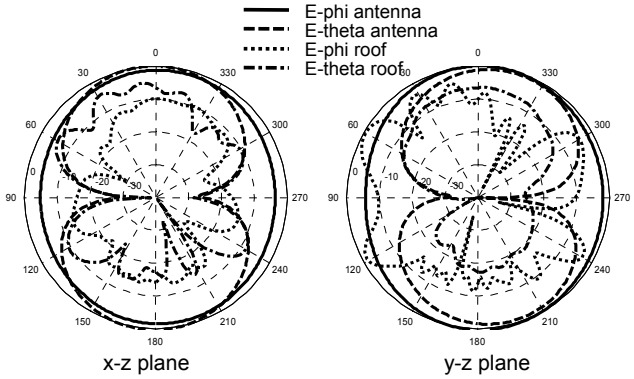


Fig. 15. Radiation pattern comparison of the antenna alone and the antenna on the roof at GPS.

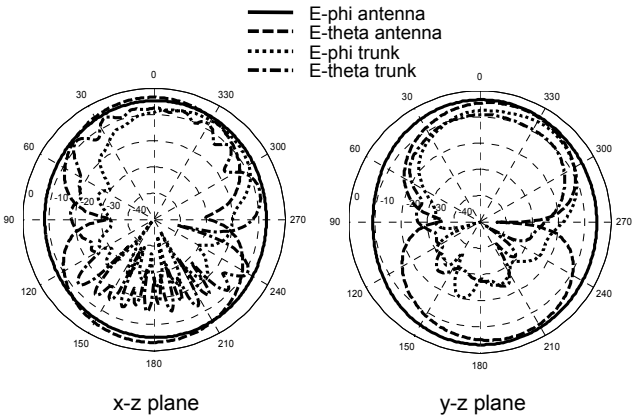


Fig. 16. Radiation pattern comparison of the antenna alone and the antenna on the trunk at GPS.

Figure 17 and Fig. 18 show the radiation pattern comparisons of the antenna and the antenna on the 4-Door and convertible automobiles. The co-polarization patterns are very similar in both cases. Especially, E-phi patterns on the y-z plane have very close values. The saw-like pattern for the automobiles is actually an expected case. Besides that, the y-z plane is wider than the x-z plane and the automobiles have more deteriorated cross-polarization patterns.

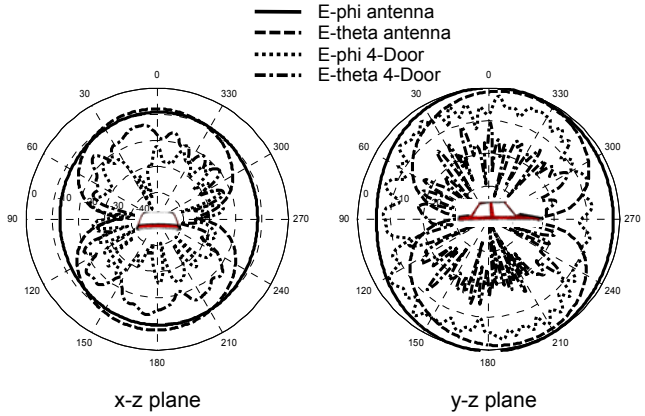


Fig. 17. Radiation pattern comparison of the antenna alone and the antenna on the 4-Door automobile at GPS.

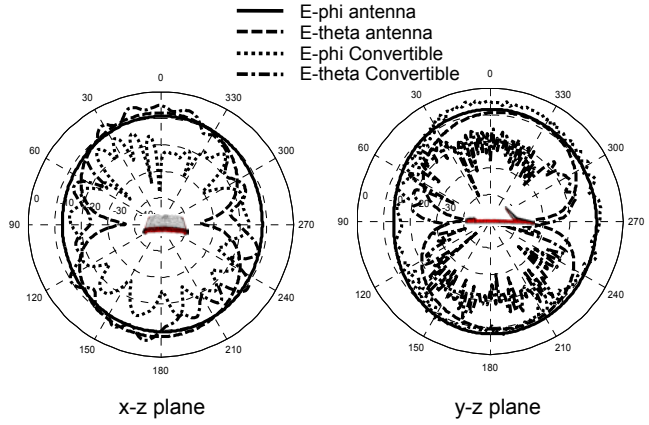


Fig. 18. Radiation pattern comparison of the antenna alone and the antenna on the convertible automobile at GPS.

## V. Conclusion

A set of hierarchical mixed-order TVFEs for tetrahedral elements up to and including 2.5 order are proposed. A wide band square slot antenna with an E-shaped tuning stub is designed using FE-BI method that employs the presented mixed order TVFEs. The antenna operates in the band 0.8 GHz – 3.35 GHz. The antenna has an average gain of 2 dB and provides circular polarization.

## Acknowledgment

The work reported herein was funded in part by the High Performance Computing Visualization Initiative under a contract from the Department of Defense.

## References

[1] G. Kumar and K. C. Gupta, "Directly coupled multiple resonator wide-band microstrip antenna," *IEEE Trans. Antennas Propagat.*, vol. AP-33, pp. 588-593, June 1985.

[2] D. M. Pozar, "Microstrip antenna coupled to a microstrip-line," *Electron. Lett.*, vol. 21, no. 2, pp. 49-50, Jan. 1985.

[3] J. Gong and J. L. Volakis, "Parametric study and design of slot-spiral antennas using an FE-BI antenna code," *Antennas and Propagation Society International Symposium*, vol. 3, pp. 2046 – 2049, 21-26 July 1996.

[4] Q. Shen, B. L. Ooi, and M. S. Leong, "A novel E-shaped broadband microstrip patch antenna," *Piers2000 Proceedings*, pp. 621, July 5th – July 14th , 2000, Boston, USA.

[5] J. Thaysen, K. B. Jakobsen, and H. R. Lenler-Eriksen, "Wideband cavity backed spiral antenna for stepped frequency ground penetrating radar," *Antennas and Propagation Society International Symposium*, vol. 1B, pp. 418 – 421, 3-8 July 2005.

[6] E. Gschwendtner, J. Parlebas, and W. Wiesbeck, "Spiral antenna with frequency-independent coplanar feed for mobile communication systems," *Antennas and Propagation Society International Symposium*, vol. 1, pp. 560 – 563, 11-16 July 1999.

[7] F. Yang, X. X. Zhang, X. Ye, and Y. Rahmat-Samii, "Wide-band E-shaped patch antennas for wireless communications," *IEEE Trans. Antennas Propagat.*, vol. 49, no. 7, pp. 1094-1100, July 2001.

[8] Y. Ge, K. P. Esselle, and T. S. Bird, "Broadband E-shaped patch antennas for 5-6 GHz wireless computer networks," *IEEE Antennas Propagat. Soc. Int. Symp. Dig.*, Columbus, OH, USA, June 2003, pp. II: 942-945.

[9] A. A. Eldek, A. Z. Elsherbeni, and C. E. Smith, "Dual-Wideband Square Slot Antenna with a U-Shaped Printed Tuning Stub for Personal Wireless Communication Systems," *Progress in Electromagnetics Research*, vol. 53, pp. 319-333, 2005.

[10] J. Y. Sze and K. L. Wong, "Bandwidth Enhancement of a Microstrip-Line-Fed Printed Wide-Slot Antenna," *IEEE Trans. Antennas Propagat.*, vol. 49, no. 7, pp. 1020-1024, July 2001.

[11] J. L. Volakis, A. Chatterjee and L. Kempel, "Finite Element Methods for Electromagnetics," *IEEE Press*, 1998.

[12] T. Karacolak and E. Topsakal, "Hierarchical Tangential Vector Finite Elements for Tetrahedra," *IEEE AP-S International Symposium and USNC/URSI Meeting*, 3-8 July 2005.

[13] L. S. Andersen and J. L. Volakis, "Accurate and efficient simulation of antennas using hierarchical mixed-order tangential vector finite elements for tetrahedral," *IEEE Trans. Antenna Propagat.*, vol. 47, pp. 1240-1243, August 1999.

[14] R X. Q. Sheng, J. M. Jin, J. M. Song, C. C. Lu, and W. C. Chew, "On the formulation of hybrid finite-element and boundary-integral method for 3D scattering," *IEEE Trans. Antennas Propagat.*, vol. 46, no. 3, pp. 303-311, March 1998.

[15] E. Topsakal, R. Kindt, K. Sertel, and J. Volakis, "Evaluation of the BICGSTAB(l) Algorithm for the Finite Element Boundary Integral Method," *IEEE Antennas Propagat. Magazine*, vol. 43, no. 6, pp. 124-131, December 2001.

**Tutku Karacolak** received the B.S. degree in electrical and electronics engineering from Bilkent University, Ankara, Turkey, in 2004, the M.S. degree in electrical engineering from Mississippi State University, Starkville, MS, in 2006, and is currently working toward the Ph.D. degree in electrical engineering at the Mississippi State University. His research interests are implantable antennas, numerical methods, antenna analysis and design.

**Erdem Topsakal** was born in Istanbul, Turkey in 1971. He received his BSc. degree in 1991, M.Sc. degree in 1993 and PhD degree in 1996 all in Electronics and Communication Engineering from Istanbul Technical University. He worked as an Assistant Professor in Electrical and Electronics Engineering Department at Istanbul Technical University between 1997 and 1998. He was a post doctoral fellow from 1998 to 2001 and an assistant research scientist from 2001 to July 2003 in Electrical Engineering and Computer Science Department of the University of Michigan. In August 2003, he joined the Electrical and Computer Engineering Department of James Worth Bagley College of Engineering at Mississippi State University as an Assistant Professor. His research areas include implantable antennas, electromagnetic theory, numerical methods, fast methods, antenna analysis and design, frequency selective surfaces/volumes, electromagnetic coupling and interference, direct and inverse scattering. He has published over 70 journal and conference papers in these areas. He received the URSI young scientist award in 1996 and NATO fellowship in 1997. He is a senior member of IEEE and an elected member of the URSI commissions B and K. He currently serves as the Vice Chair of the Mississippi Academy of Sciences and Associate Editor in Chief of the ACES journal.